

Vertical Self-Assembly of Polarized Phage Nanostructure for Energy Harvesting

Ju-Hyuck Lee,^{†,‡,⊥,¶} Ju Hun Lee,^{†,‡,⊥} Jun Xiao,[§] Malav S. Desai,^{†,‡} Xiang Zhang,^{§,||} and Seung-Wuk Lee^{*,†,‡,||}

[†]Department of Bioengineering, University of California, Berkeley, California 94720, United States

[‡]Biological Systems and Engineering Division, Lawrence Berkeley National Laboratory, Berkeley, California 94720, United States

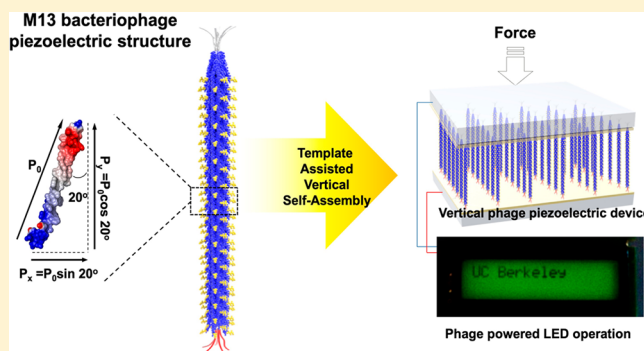
[§]Nanoscale Science and Engineering Center, University of California, Berkeley, California 94720, United States

^{||}Materials Sciences Division, Lawrence Berkeley National Laboratory, Berkeley, California 94720, United States

Supporting Information

ABSTRACT: Controlling the shape, geometry, density, and orientation of nanomaterials is critical to fabricate functional devices. However, there is limited control over the morphological and directional characteristics of presynthesized nanomaterials, which makes them unsuitable for developing devices for practical applications. Here, we address this challenge by demonstrating vertically aligned and polarized piezoelectric nanostructures from presynthesized biological piezoelectric nanofibers, M13 phage, with control over the orientation, polarization direction, microstructure morphology, and density using genetic engineering and template-assisted self-assembly process. The resulting vertically ordered structures exhibit strong unidirectional polarization with three times higher piezoelectric constant values than that of in-plane aligned structures, supported by second harmonic generation and piezoelectric force microscopy measurements. The resulting vertically self-assembled phage-based piezoelectric energy harvester (PEH) produces up to 2.8 V of potential, 120 nA of current, and 236 nW of power upon 17 N of force. In addition, five phage-based PEH integrated devices produce an output voltage of 12 V and an output current of 300 nA, simply by pressing with a finger. The resulting device can operate light-emitting diode backlights on a liquid crystal display. Our approach will be useful for assembling many other presynthesized nanomaterials into high-performance devices for various applications.

KEYWORDS: M13 bacteriophage, self-assembly, polarization, piezoelectricity, energy harvesting



Control of shape, geometry, density, and orientation during nanomaterial assembly is critical for fabricating meso- and microscale devices, and for applications.^{1–6} Especially, vertically grown one-dimensional nanostructures have a great potential in many applications in optics, electronics, energy, and sensing. Various techniques including chemical and physical vapor deposition have been utilized to synthesize carbon or inorganic materials with defined diameters and morphologies.^{7–10} The resulting vertically grown nanomaterials with controlled crystallographic orientations exhibit enhanced performance in optical lasing, energy harvesting, and sensing.^{5,11–15} Although meniscus-induced material assembly or external field-induced polarization (i.e., magnetic and electric fields) has been applied to fabricate vertically ordered nanostructures using presynthesized nanowires and nanotubes,^{16,17} it is still challenging to control their geometry, orientation, and polarization. Biological materials have a great potential to develop programmable synthesis of desired nanostructures with specific shape, orientation, and

geometry.^{18–21} Sequence specific DNAs/RNAs, antibody–antigen pairs, or bioconjugation can be used to tether and organize target materials on substrates.^{22–24} However, synthesizing biomaterials with specific functions including optical, electrical, and mechanical functions together with specific geometry and polarization is still challenging and very limited. Here, we report the self-assembly of vertically aligned biological nanostructures that are programmed to convert mechanical stimulation to electric energy. We use a rod-shaped M13 bacteriophage (phage) as a piezoelectric biomaterial and engineer its tail coat proteins to immobilize it on target substrates. We then use template-induced capillary force to vertically self-assemble phage nanostructures. Resulting vertically aligned phage exhibit unidirectional polarization, which was evidenced by second harmonic generation spectroscopy

Received: February 7, 2019

Revised: March 13, 2019

Published: March 15, 2019

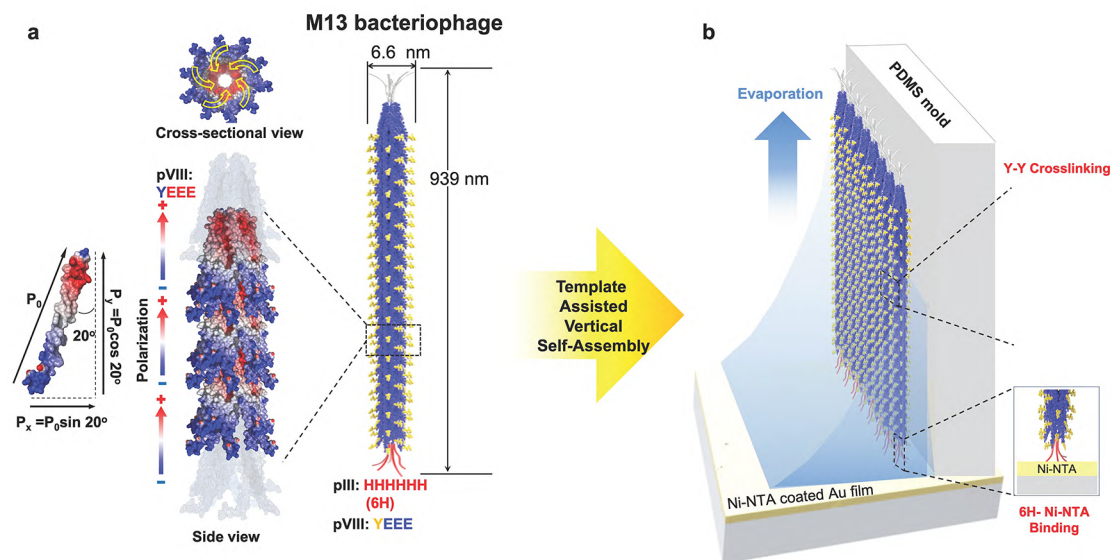


Figure 1. Schematic of piezoelectricity on vertically aligned M13 phage. (a) M13 phage is a long rodlike bacterial virus, 939 ± 20 nm ($n = 25$) in length and 6.6 nm in diameter. A cross-sectional view of the M13 phage to show 5-fold rotational symmetry (with 2-fold screw symmetry). The M13 phage is covered by 2700 pVIII coat proteins. The pVIII coat protein has an $\sim 20^\circ$ tilt angle with respect to the phage long axis. The colors of the molecular surface indicate positive (red), neutral (white), and negative (blue) electrostatic potentials. The M13 phages are engineered in the minor and major coat protein. (i) The minor coat proteins are engineered with a 6-histidine tag (6H) to produce strong specific binding with the Ni-NTA/Au electrode. (ii) pVIII major coat proteins are engineered with YEEE at the N-terminal. The tyrosine (Y) forms dityrosine (Y–Y) cross-links between phages and the three glutamate can produce strong polarization in axial direction. (b) The resulting phage can vertically self-assemble into unidirectionally polarized phage nanostructure assisted by templates. Insets show the structure of Y–Y cross-links between phages in the major coat protein pVIII and 6H–Ni–NTA binding in the minor coat protein pIII.

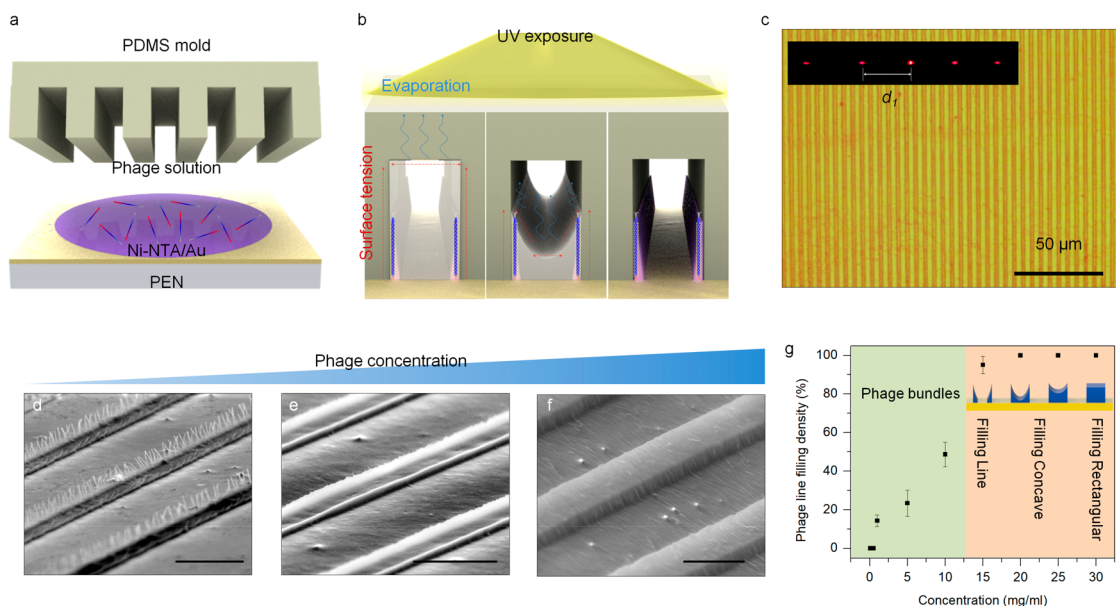


Figure 2. Formation of vertically aligned phage. (a) Schematic diagram of fabrication process of vertically aligned phage. A micropatterned PDMS mold is brought into contact with the substrate surface uniformly covered by phage solution. (b) As the solvent evaporates, capillary force is induced due to surface tension and it causes the phages to self-assemble into bundles that stand up vertically along the pattern walls as they dry (middle). (c) Optical image of the phage nanostructures over large area. Inset: laser diffraction pattern obtained from the patterned phage. (d–f) Scanning electron microscope (SEM) images of the patterned M13 phages depending on the concentration of phage solution. The vertically aligned M13 phages form individual phage bundles, line, and rectangular shapes as the phage concentration increases. (g) Vertically aligned phage line filling density versus phage concentration.

and piezo-responsive microscopy techniques. Furthermore, we genetically engineered them to enhance their mechanical durability through tyrosine(Y)-mediated cross-links. The vertically aligned phage-based piezoelectric energy harvester (PEH) that we fabricated generates up to 2.8 V of potential,

120 nA of current, and 236 nW of power with 17 N of force. In addition, five series-connected PEH devices produced an output voltage of 12 V, while parallel PEHs produced an output current of 300 nA, simply by pressing with a finger. The resulting device can operate light-emitting diode backlights on

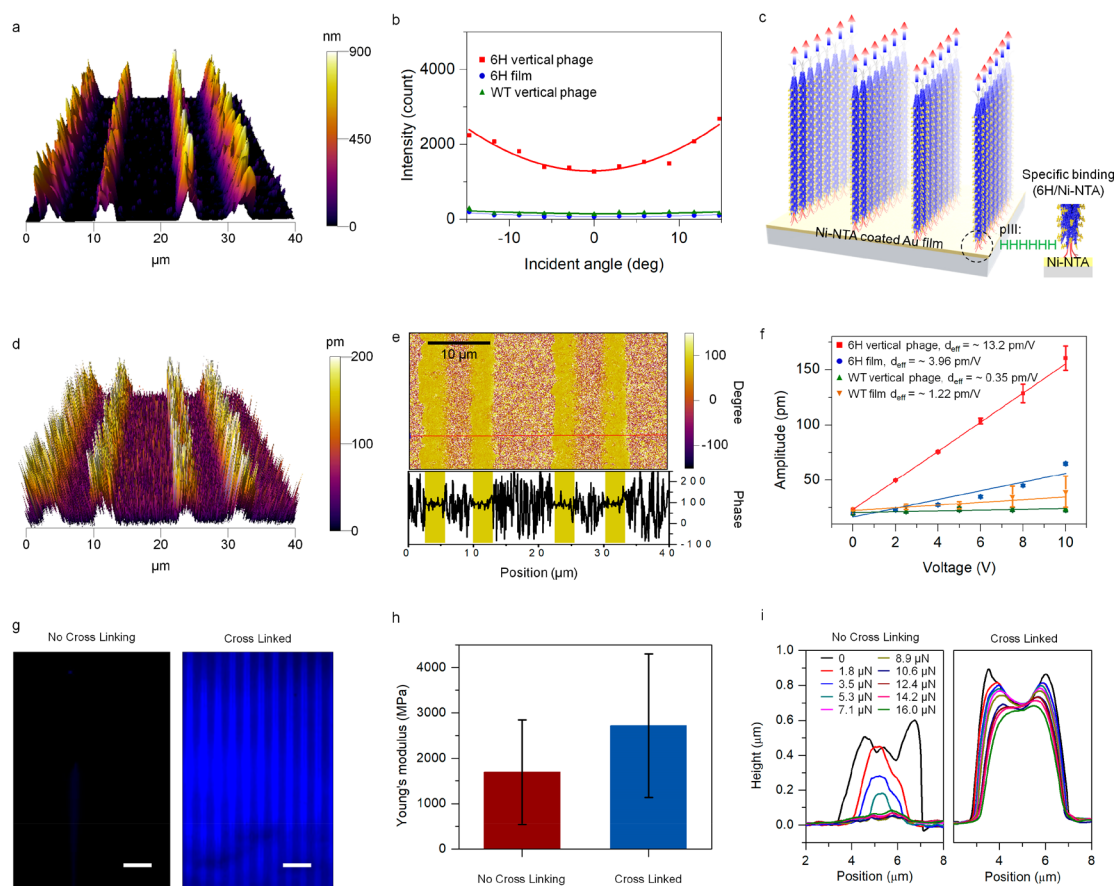


Figure 3. Characterization of polarization and mechanical properties of vertically aligned phage. (a) 3D-AFM topography image of vertically aligned phages. (b) Angle-dependent SHG intensity in vertically aligned engineered phage, randomly aligned engineered phage and vertically aligned wild-type phage. In the vertically aligned engineered phage, strong SHG intensity is observed and the intensity increases symmetrically with greater tilted incidence, which indicates the presence of vertically aligned dipoles. (c) The direction of polarization of the vertically aligned phage with specific binding between 6H tag on phage tail and Ni-NTA substrate. (d) Piezoresponse force microscope (PFM) amplitude image corresponding to the 3D-AFM topography image. (e) The PFM phase image of vertically aligned phage exhibits unidirectional polarization in the out-of-plane direction. (f) Comparison of out-of-plane PFM amplitude versus applied voltage for genetically engineered coat proteins pVIII along aligned direction. Error bars indicate one standard deviation. (g) Fluorescence optical image of phage pattern with/without cross-linking. Scale bar: 20 μm . (h) The Young's modulus characterization of the phage pattern with and without cross-linking. (i) Representative AFM height profiles after application of shear force using AFM tip on the patterned phage with/without cross-linking.

a liquid crystal display (LCD). Our programmable biomaterial design to fabricate the vertically oriented nanostructures with control over polarization and orientation using presynthesized nanomaterials will greatly expand the application of nanomaterials in mesoscale material assembly and device fabrication.

Results. M13 phage is a long rodlike bacterial virus, 939 ± 20 nm ($n = 25$, genetically engineered phage in this study) in length and 6.6 nm in diameter (Figure 1a,b). Because of its rodlike shape with monodispersity, genetic and chemical flexibility to display functional motifs and ability to self-assemble into various hierarchical structures, M13 phages have been utilized to create various nanostructures for applications including biosensors, tissue regeneration, and energy storage and generating materials.^{21,25,26} Furthermore, M13 phage itself exhibits piezoelectricity originating from its 2-fold symmetry, and the 5-fold rotational arrangement of its major coat proteins²⁷ (Figure 1b). Previously, using piezo-responsive force microscopy (PFM), we showed in-plane and out-of-plane piezoelectric responses upon application of electric fields on an in-plane aligned monolayer phage film, which corresponds to the radial and axial piezoelectric components of M13 phage, respectively. Because of the 20° tilted angle of the pVIII

protein, the piezoelectricity in the axial direction of the M13 phages is expected to be three times stronger than that in the radial direction^{28–30} (Figure 1c). The polarization of the axial and radial component of a single pVIII (net polarization: P_0) is expected to be 0.94 P_0 and 0.34 P_0 , respectively. To enhanced piezoelectric energy generation from the phage-based devices, it is critical to construct vertically aligned phage nanostructures with polarization control. We approach this problem by genetically engineering M13 phage to express multiple functional peptides to control their geometry, electrical, and mechanical functions in a modular manner. First, to polarize the binding of phage on the substrate, we engineered the M13 phage with hexa-histidine (6H) at the N-terminal of the minor coat protein (pIII). 6H can bind strongly to nickel–nitrilotriacetic acid (Ni-NTA) modified substrate³¹ (Figure 1a,e, and Supplementary Figures 1). Second, to enhance their piezoelectrical performance we fused three glutamates (3E) at the N-terminal of pVIII major coat protein to enhance the dipole strength of the protein (Figure 1d). Lastly, to enhance the mechanical stability of the vertically aligned phage nanostructures, we expressed a Tyrosine (Y) residue at the

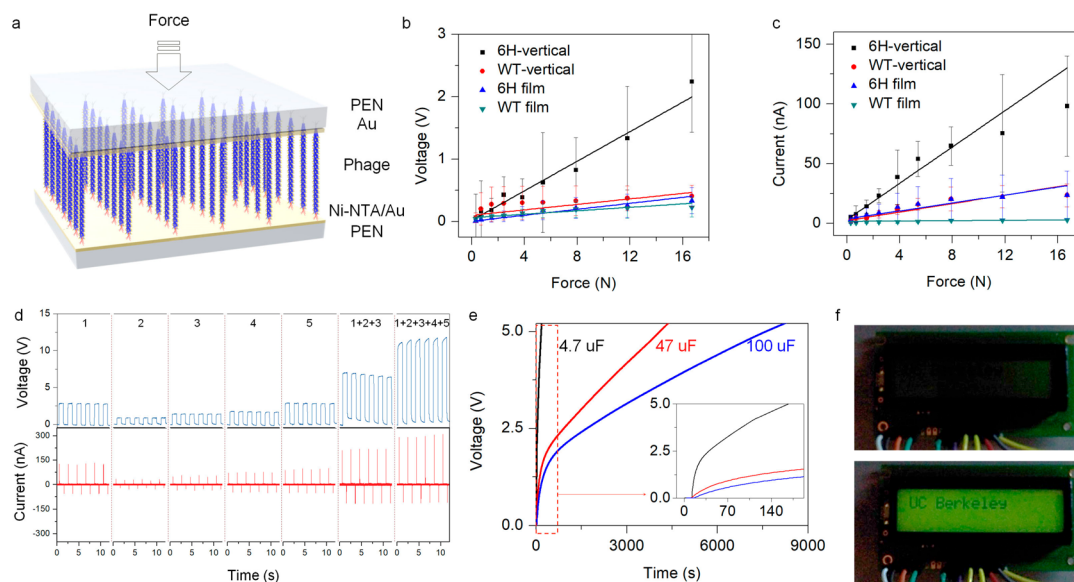


Figure 4. Characterization of vertically aligned phage based piezoelectric energy harvesters. (a) Schematic illustration of vertically aligned engineered phage piezoelectric energy harvesters. (b,c) Comparison of output voltages and output currents by applied forces along alignment directions. Error bars indicate one standard deviation. (d) Constructive voltage (blue) and current (red) outputs by serial connection of individual devices. (e) Charging curves of capacitors collecting energy from phage-based piezoelectric device. (f) Operation of LED using 100 μF capacitor using serially connected five devices (top), and photo image of turning an LED back light on the LCD panel using the device (bottom).

N-terminal in order to form Y–Y cross-linkage³² between neighboring phages through UV illumination (Figure 1d,e).

We fabricated vertically aligned nanostructures using the engineered phages and by controlling interfacial forces. In order to create the vertically aligned phage nanostructures, we use a micropatterned polydimethylsiloxane (PDMS) mold as a template. Typically, phage solution is deposited on a Ni–NTA-coated substrate (Figure 1e and 2a). A PDMS mold is applied on top of the solution, which is then allowed to dry. As the solvent in the phage solution evaporates, it induces an upward capillary force on the Ni–NTA-bound phage. The upward force causes phages to self-assemble into a monolayer of vertically aligned bundles (Figure 1e and 2b). After the sample is fully dry, the PDMS mold is removed to achieve free-standing nanostructures. Furthermore, we can enhance the mechanical properties of phage nanostructures by cross-linking them through UV exposure as they dry (Figure 1e). Using the capillary force driven template-assembly method, we can fabricate vertically aligned phage nanostructures over large areas (Figure 2c). We can create various morphologies and patterns of the vertically aligned phage nanostructures using this method. With a concentration control, we can tune vertically aligned nanostructure morphology from individual phage bundles to rows of rectangular shapes using a PDMS line pattern mold with 5 μm spacing (Figure 2d–g and Supplementary Figure 2). At low phage concentrations (10 mg mL^{-1}), vertically aligned individual phage nanobundles are observed. (Figure 2d). As the phage concentration is increased (15 mg mL^{-1}), the density of the phage bundles increases until a line of vertically standing phage is observed as shown in Figure 2e. The height of the line pattern is about ~ 900 nm, which is commensurate with the length of an individual phage (880 nm) and confirms that the vertically aligned nanostructures consist of a monolayer of phage (Supplementary Figure 3a). As the phage concentration is further increased (20–30 mg mL^{-1}), we observe that the shape of the patterns changes to concave, followed by rectangular shapes by filling up the

PDMS templates (Figure 2f and Supplementary Figure 3). In addition, the interspacing of the vertically aligned phage nanostructures can be easily tuned by applying PDMS molds with different spacing (Supplementary Figure 4 and 5).

We verified unidirectional polarization of phages in the vertically aligned nanostructures using second harmonic generation (SHG) and atomic force microscopy (AFM). Once we confirmed that our nanostructures are composed of vertically aligned phage monolayer (Figure 3a), we characterized the dipole orientation of phage using SHG measurements (Figure 3b and Supplementary Figure 6). The phage nanostructures exhibited strong SHG signals resulting from unidirectionally polarized structure, while the control samples (in-plane aligned engineered phage and vertically aligned wildtype (WT) phage) exhibited weak SHG signals. We also found enhancement of SHG signal by applying tilted incident³³ beam corresponding to the presence of out-of-plane dipole of the patterned phage. The SHG results confirmed that the fabricated phage patterns were unidirectionally polarized due to the specific binding between 6-His tag on phage tail proteins and the Ni–NTA substrate (Figure 3c). We then characterized the piezoelectric properties of vertically aligned phage nanostructures by measuring their mechanical responses to the applied electric field using PFM. We observed strong piezo-response corresponding to the out-of-plane polarization from the vertically aligned phage nanostructures (Figure 3d). In addition, the assembled phages also exhibited unidirectionally oriented piezoelectric polarization with an effective vertical piezoelectric coefficient, d_{eff} of 13.2 pm V^{-1} (Figure 3e). On the other hand, the vertically aligned WT phage control samples exhibited a relatively weak piezo-response due to random, antiparallel orientation (Supplementary Figure 7).²⁷ In fact, the piezoelectric response of vertically aligned WT phages was even lower than that of 6H-film and WT control films. The d_{eff} of drop-cast engineered phage, vertically aligned WT phage, and drop-cast WT phage films were 3.96, 1.22, and 0.35 pm V^{-1} , respectively (Figure 3f and Supplementary

Figures 8 and 9). These measurements are in reasonable agreement with the SHG results. In the case of concave-structured phage nanostructures, we observed stronger piezoelectric response from the edges than the middle, which showed that capillary forces are enhanced near the PDMS interfaces (Supplementary Figure 10). Because the resulting vertically aligned phage nanostructures are intended for the fabrication of piezoelectric devices, the mechanical stability is also critical. Therefore, we enhanced the mechanical properties of the vertically aligned phages through dityrosine cross-links between neighboring phages. After UV illumination, the phage patterns exhibited strong blue fluorescence emission indicating successful dityrosine cross-link formation between the phages (Figure 3g). The resulting cross-linked phage structure exhibited a 2-fold enhancement of Young's modulus compared to non-cross-linked phage structures. (Figure 3h). In addition, when we deformed the vertically aligned phages with a stepwise increase of shear force using an AFM tip, we observe that the cross-linked vertically aligned phage structures were more stable compared to non-cross-linked control, which began to deform at 10 μN force (Figure 3i). We expected that the mechanically enhanced phage structures will exhibit outstanding device performance and stability.

We fabricated piezoelectric energy harvesters (PEHs) using the resulting unipolarized vertically aligned phages (Figure 4). We first assembled vertically aligned and unipolarized phage on a Au/Cr coated flexible PEN substrate. We then assembled another Au/Cr coated PEN substrate as a top electrode. The resulting vertically aligned phage-based devices generated electricity upon application of mechanical force. We measured the open-circuit voltage (V_{oc}) and short-circuit current (I_{sc}) from the PEHs by periodic compressive forces (see detail procedure in Supporting Information). The peak voltage reached 2.8 V, the current reached 120 nA and the power reached 236 nW with 17 N of force (Supplementary Figures 11 and 12). Switching polarity measurement confirmed that the observed signals were generated by the PEH (Supplementary Figure 13).³⁴ The generated output power from the phage PEHs were improved by about 20-fold and 25-fold compared to those associated with the vertically aligned WT phage and drop-cast engineered phage film-based PEH, respectively (Figure 4b,c and Supplementary Figure 14). The output power of the PEHs can be improved by integrating multiple PEHs into a single device (Supplementary Figure 15). A series connection increases the output voltage and a parallel connection increases the output current.³⁵ We fabricated five phage-based PEHs and characterized the output voltages and currents for each PEH and integrated PEHs (Figure 4d,e). The series connected PEHs produced an output voltage of ~ 12 V, while parallel PEHs produced an output current of ~ 300 nA, simply by pressing with a finger. The output voltage and current were approximately the sum of the output performances of the individual PEHs. These results also confirm that the measured signal was generated by the PEHs. We showed the practicality of our PEH devices integrated with energy storage by charging capacitors via a rectifier circuit (Figure 4f). When we used a series connected PEH device, the 4.7, 47, and 100 μF capacitors reached 5 V at 140, 4000, and 8000 s, respectively. Using the resulting PEH device with 100 μF capacitor, we powered a light-emitting diode backlight for a liquid crystal display panel to show "UC Berkeley" (Figure 4g and Supplementary Figure 15). Devices made using mechanically robust phage nanostructures with high piezoelectricity,

through control over phage direction and polarity, provide with a renewable and biocompatible source of energy for future biomedical applications.

Conclusion. The self-assembly of presynthesized nanomaterials with control over shape, geometry, orientation and pattern can significantly expand the function of nanomaterials in various applications including optics, sensing, energy storage and harvesting. Our approach has allowed us to control the density, shape, orientation and polarization of the M13 phage, a presynthesized nanomaterial, and the resulting phage nanostructures exhibited significantly enhanced piezoelectric properties through unidirectional polarization. The vertically aligned phage-based PEHs can generate 2.8 V of voltage and 120 nA of current, which is more than 100 times higher electrical power (W) than 0.4 V of voltage and 6 nA of current generated from previously reported in-plane aligned phages. Furthermore, the five phage-PEH integrated device produces an output voltage of 12 V and current of 300 nA simply by pressing with a finger. To our knowledge, this is the highest output of any biomaterial-based piezoelectric energy harvester reported so far.^{27,36,37} Our approach can be extended to control the nanostructure of various organic/inorganic materials for the development of a variety of high-performance functional applications.^{37,38}

Methods and Materials. Genetic Engineering of Phage.

We constructed desired engineered phages using recombinant DNA engineering methods. Briefly, YEEE peptide with spacers was first expressed between the first and the fourth residues at the N-terminal of wild-type phage major coat protein 8 (pVIII). Additionally, a 6H tag was engineered at the N-terminal of phage minor coat protein 3 (pIII) with a spacer (Gly-Gly-Gly-Ser). The engineered phages were amplified through bacterial host cell infection and purification. DNA sequences were confirmed after amplification.

Formation of Vertical Phage Structure. Phage solutions ($0.1\text{--}30$ mg mL⁻¹) with 0.05 mM Ru(II)bpy₃²⁺ and 0.5 mM ammonium persulfate were applied on the Ni-NTA/Au substrate. Then, the PDMS micropattern mold was contacted with the substrate surface covered by phage solution. The phage solution was exposed with UV light for 0–60 min and fully dried. The PDMS mold was carefully removed and the final product was kept in a desiccator until use.

Microstructure Analysis. Optical microscopic images were collected using an IX71 Inverted Microscope (Olympus, Tokyo, Japan) equipped with a digital CCD camera, RETIGA 2000 (QIMAGING) and STC-MC152USB (SENTECH America). Scanning electron microscopy (SEM) images were collected using a scanning electron microscope (FEI, Quanta 3D FEG). Atomic force microscopy (AFM) images and piezoresponsive force microscopy (PFM) images were collected using MFP3D AFM (Asylum Research, Santa Barbara, CA). A Tap150Al-G (Budgetsensors) tip with a nominal spring constant of ~ 5 N m⁻¹ and a free-air resonance frequency of ~ 150 kHz, and a AC240TM-R3 (Asylum research, Santa Barbara, CA) tip with nominal spring constant 2 N m⁻¹ and a free-air resonance frequency of ~ 70 kHz were used for AFM and PFM images, respectively.

Second Harmonic Generation (SHG) Characterization. We characterized the unipolarization of the vertically aligned phage using incident angle-dependent SHG spectroscopy. We generated the p-polarized excitation wavelength (900–1300 nm) using a Ti:sapphire oscillator (Chameleon Compact OPO-Vis, Coherent Inc., USA). Collimated p-polarized (along

the horizontal direction) beam with ~ 1 mm spot size was illuminated on the objective back aperture ($D = 7.6$ mm). The laser beam was focused on the vertically aligned phage samples. The beam position was scanned along x -axis with a motorized stage to generate variable oscillating vertical electrical field, as reported in ref 33. The SHG signal was obtained through the same objective lens.

Piezoelectric Device Fabrication. The vertically aligned phages were fabricated on the Ni-NTA/Au-coated polyethylene naphthalate (PEN) substrate using 15 mg mL^{-1} of phage solution and PDMS micropattern with a width of $5 \mu\text{m}$. After the completion of fabrication process, PDMS was spin coated as a protection layer on the vertically aligned phage. Once polymerized, another Cr/Au coated PEN substrate was placed on the PDMS layer as the top electrode.

Piezoelectric Energy Harvester Characterization. The phage-based PEH was mounted on a dynamic mechanical test system (Electroforce 3200, Bose, MN) and a predefined displacement was applied. Force was monitored with a 50 lb-f load cell and displacement was adjusted until the desired amount of force was reached. A programmable electrometer (Keithley model 6514) and a low-noise current preamplifier (Stanford Research System model SR570) were used to acquire open-circuit voltage and short circuit current, respectively.

■ ASSOCIATED CONTENT

Supporting Information

The Supporting Information is available free of charge on the ACS Publications website at DOI: 10.1021/acs.nanolett.9b00569.

Additional supporting Figures S1–S15 (PDF)

■ AUTHOR INFORMATION

Corresponding Author

*E-mail. leesw@berkeley.edu.

ORCID

Xiang Zhang: 0000-0002-3272-894X

Seung-Wuk Lee: 0000-0002-0501-8432

Present Address

[#](J.-H.L.) Department of Energy Science and Engineering, Daegu Gyeongbuk Institute of Science and Technology (DGIST), Daegu 42988, Republic of Korea.

Author Contributions

[†]J.-H. L. and J.H.L. contributed equally to this work.

Notes

The authors declare no competing financial interest.

■ ACKNOWLEDGMENTS

This work was supported by the U.S. Army Engineering Research Development Center (W912HZ-14-2-0027). This work was also supported by Tsinghua Berkeley Shenzhen Institute Fund.

■ REFERENCES

- (1) Demers, L. M.; Ginger, D. S.; Park, S. J.; Li, Z.; Chung, S. W.; Mirkin, C. A. Direct Patterning of Modified Oligonucleotides on Metals and Insulators by Dip-Pen Nanolithography. *Science* **2002**, *296*, 1836–8.
- (2) Adler-Abramovich, L.; Aronov, D.; Beker, P.; Yevnin, M.; Stempler, S.; Buzhansky, L.; Rosenman, G.; Gazit, E. Self-Assembled

Arrays of Peptide Nanotubes by Vapour Deposition. *Nat. Nanotechnol.* **2009**, *4*, 849–854.

- (3) Wu, W. Z.; Wen, X. N.; Wang, Z. L. Taxel-Addressable Matrix of Vertical-Nanowire Piezotronic Transistors for Active and Adaptive Tactile Imaging. *Science* **2013**, *340*, 952–957.

- (4) Modi, A.; Koratkar, N.; Lass, E.; Wei, B. Q.; Ajayan, P. M. Miniaturized Gas Ionization Sensors Using Carbon Nanotubes. *Nature* **2003**, *424*, 171–174.

- (5) Chan, C. K.; Peng, H. L.; Liu, G.; McIlwrath, K.; Zhang, X. F.; Huggins, R. A.; Cui, Y. High-Performance Lithium Battery Anodes Using Silicon Nanowires. *Nat. Nanotechnol.* **2008**, *3*, 31–35.

- (6) Takei, K.; Takahashi, T.; Ho, J. C.; Ko, H.; Gillies, A. G.; Leu, P. W.; Fearing, R. S.; Javey, A. Nanowire Active-Matrix Circuitry for Low-Voltage Macroscale Artificial Skin. *Nat. Mater.* **2010**, *9*, 821–826.

- (7) Wang, X. D.; Summers, C. J.; Wang, Z. L. Large-Scale Hexagonal-Patterned Growth of Aligned ZnO Nanorods for Nano-Optoelectronics and Nanosensor Arrays. *Nano Lett.* **2004**, *4*, 423–426.

- (8) Kong, Y. C.; Yu, D. P.; Zhang, B.; Fang, W.; Feng, S. Q. Ultraviolet-Emitting ZnO Nanowires Synthesized by a Physical Vapor Deposition Approach. *Appl. Phys. Lett.* **2001**, *78*, 407–409.

- (9) Tomioka, K.; Yoshimura, M.; Fukui, T. A Iii-V Nanowire Channel on Silicon for High-Performance Vertical Transistors. *Nature* **2012**, *488*, 189–192.

- (10) Futaba, D. N.; Hata, K.; Yamada, T.; Hiraoka, T.; Hayamizu, Y.; Kakudate, Y.; Tanaike, O.; Hatori, H.; Yumura, M.; Iijima, S. Shape-Engineerable and Highly Densely Packed Single-Walled Carbon Nanotubes and Their Application as Super-Capacitor Electrodes. *Nat. Mater.* **2006**, *5*, 987–994.

- (11) Ren, Z. F.; Huang, Z. P.; Xu, J. W.; Wang, J. H.; Bush, P.; Siegal, M. P.; Provencio, P. N. Synthesis of Large Arrays of Well-Aligned Carbon Nanotubes on Glass. *Science* **1998**, *282*, 1105–1107.

- (12) Suzuki, H.; Kaneko, T.; Shibuta, Y.; Ohno, M.; Maekawa, Y.; Kato, T. Wafer-Scale Fabrication and Growth Dynamics of Suspended Graphene Nanoribbon Arrays. *Nat. Commun.* **2016**, *7*, 11797.

- (13) Zhang, S. C.; Kang, L. X.; Wang, X.; Tong, L. M.; Yang, L. W.; Wang, Z. Q.; Qi, K.; Deng, S. B.; Li, Q. W.; Bai, X. D.; et al. Arrays of Horizontal Carbon Nanotubes of Controlled Chirality Grown Using Designed Catalysts. *Nature* **2017**, *543*, 234–238.

- (14) Hannon, J. B.; Kodambaka, S.; Ross, F. M.; Tromp, R. M. The Influence of the Surface Migration of Gold on the Growth of Silicon Nanowires. *Nature* **2006**, *440*, 69–71.

- (15) Kuykendall, T.; Pauzauskie, P. J.; Zhang, Y. F.; Goldberger, J.; Sirbuly, D.; Denlinger, J.; Yang, P. D. Crystallographic Alignment of High-Density Gallium Nitride Nanowire Arrays. *Nat. Mater.* **2004**, *3*, 524–528.

- (16) Beardslee, J. A.; Sadtler, B.; Lewis, N. S. Magnetic Field Alignment of Randomly Oriented, High Aspect Ratio Silicon Microwires into Vertically Oriented Arrays. *ACS Nano* **2012**, *6*, 10303–10310.

- (17) Baker, J. L.; Widmer-Cooper, A.; Toney, M. F.; Geissler, P. L.; Alivisatos, A. P. Device-Scale Perpendicular Alignment of Colloidal Nanorods. *Nano Lett.* **2010**, *10*, 195–201.

- (18) Reches, M.; Gazit, E. Controlled Patterning of Aligned Self-Assembled Peptide Nanotubes. *Nat. Nanotechnol.* **2006**, *1*, 195–200.

- (19) Jin, J. H.; Hassanzadeh, P.; Perotto, G.; Sun, W.; Brenckle, M. A.; Kaplan, D.; Omenetto, F. G.; Rolandi, M. A Biomimetic Composite from Solution Self-Assembly of Chitin Nanofibers in a Silk Fibroin Matrix. *Adv. Mater.* **2013**, *25*, 4482–4487.

- (20) O'Leary, L. E. R.; Fallas, J. A.; Bakota, E. L.; Kang, M. K.; Hartgerink, J. D. Multi-Hierarchical Self-Assembly of a Collagen Mimetic Peptide from Triple Helix to Nanofibre and Hydrogel. *Nat. Chem.* **2011**, *3*, 821–828.

- (21) Chung, W. J.; Oh, J. W.; Kwak, K.; Lee, B. Y.; Meyer, J.; Wang, E.; Hexemer, A.; Lee, S. W. Biomimetic Self-Templating Supramolecular Structures. *Nature* **2011**, *478*, 364–368.

- (22) Demers, L. M.; Park, S. J.; Taton, T. A.; Li, Z.; Mirkin, C. A. Orthogonal Assembly of Nanoparticle Building Blocks on Dip-Pen

Nanolithographically Generated Templates of DNA. *Angew. Chem., Int. Ed.* **2001**, *40*, 3071–3073.

(23) Zhang, S. G.; Yan, L.; Altman, M.; Lassle, M.; Nugent, H.; Frankel, F.; Lauffenburger, D. A.; Whitesides, G. M.; Rich, A. Biological Surface Engineering: A Simple System for Cell Pattern Formation. *Biomaterials* **1999**, *20*, 1213–1220.

(24) Soong, R. K.; Bachand, G. D.; Neves, H. P.; Olkhovets, A. G.; Craighead, H. G.; Montemagno, C. D. Powering an Inorganic Nanodevice with a Biomolecular Motor. *Science* **2000**, *290*, 1555–1558.

(25) Lee, S. W.; Mao, C. B.; Flynn, C. E.; Belcher, A. M. Ordering of Quantum Dots Using Genetically Engineered Viruses. *Science* **2002**, *296*, 892–895.

(26) Lee, J. H.; Warner, C. M.; Jin, H. E.; Barnes, E.; Poda, A. R.; Perkins, E. J.; Lee, S. W. Production of Tunable Nanomaterials Using Hierarchically Assembled Bacteriophages. *Nat. Protoc.* **2017**, *12*, 1999–2013.

(27) Lee, B. Y.; Zhang, J. X.; Zueger, C.; Chung, W. J.; Yoo, S. Y.; Wang, E.; Meyer, J.; Ramesh, R.; Lee, S. W. Virus-Based Piezoelectric Energy Generation. *Nat. Nanotechnol.* **2012**, *7*, 351–356.

(28) Minary-Jolandan, M.; Yu, M. F. Nanoscale Characterization of Isolated Individual Type I Collagen Fibrils: Polarization and Piezoelectricity. *Nanotechnology* **2009**, *20*, 085706.

(29) Shin, D. M.; Han, H. J.; Kim, W. G.; Kim, E.; Kim, C.; Hong, S. W.; Kim, H. K.; Oh, J. W.; Hwang, Y. H. Bioinspired Piezoelectric Nanogenerators Based on Vertically Aligned Phage Nanopillars. *Energy Environ. Sci.* **2015**, *8*, 3198–3203.

(30) Vasilev, S.; Zelenovskiy, P.; Vasileva, D.; Nuraeva, A.; Shur, V. Y.; Kholkin, A. L. Piezoelectric Properties of Diphenylalanine Microtubes Prepared from the Solution. *J. Phys. Chem. Solids* **2016**, *93*, 68–72.

(31) Kelly, D. F.; Dukovski, D.; Walz, T. Monolayer Purification: A Rapid Method for Isolating Protein Complexes for Single-Particle Electron Microscopy. *Proc. Natl. Acad. Sci. U. S. A.* **2008**, *105*, 4703–4708.

(32) Sando, L.; Kim, M.; Colgrave, M. L.; Ramshaw, J. A. M.; Werkmeister, J. A.; Elvin, C. M. Photochemical Crosslinking of Soluble Wool Keratins Produces a Mechanically Stable Biomaterial That Supports Cell Adhesion and Proliferation. *J. Biomed. Mater. Res., Part A* **2010**, *95a*, 901–911.

(33) Lu, A. Y.; Zhu, H. Y.; Xiao, J.; Chuu, C. P.; Han, Y. M.; Chiu, M. H.; Cheng, C. C.; Yang, C. W.; Wei, K. H.; Yang, Y. M.; et al. Janus Monolayers of Transition Metal Dichalcogenides. *Nat. Nanotechnol.* **2017**, *12*, 744–749.

(34) Yang, R. S.; Qin, Y.; Dai, L. M.; Wang, Z. L. Power Generation with Laterally Packaged Piezoelectric Fine Wires. *Nat. Nanotechnol.* **2009**, *4*, 34–39.

(35) Wu, W. Z.; Wang, L.; Li, Y. L.; Zhang, F.; Lin, L.; Niu, S. M.; Chenet, D.; Zhang, X.; Hao, Y. F.; Heinz, T. F.; et al. Piezoelectricity of Single-Atomic-Layer MoS₂ for Energy Conversion and Piezotronics. *Nature* **2014**, *514*, 470–474.

(36) Nguyen, V.; Zhu, R.; Jenkins, K.; Yang, R. S. Self-Assembly of Diphenylalanine Peptide with Controlled Polarization for Power Generation. *Nat. Commun.* **2016**, *7*, 13566.

(37) Lee, J. H.; Heo, K.; Schulz-Schonbagen, K.; Lee, J. H.; Desai, M. S.; Jin, H. E.; Lee, S. W. Diphenylalanine Peptide Nanotube Energy Harvesters. *ACS Nano* **2018**, *12*, 8138–8144.

(38) Jin, H.-E.; Jang, J.; Chung, J.; Lee, H. J.; Wang, E.; Lee, S.-W.; Chung, W.-J. Biomimetic Self-Templated Hierarchical Structures of Collagen-Like Peptide Amphiphiles. *Nano Lett.* **2015**, *15*, 7138–7145.